Macromolecules

ARTICLE

pubs.acs.org/Macromolecules

Thermal and Strain-Induced Chain Ordering in Lactic Acid Stereocopolymers: Influence of the Composition in Stereomers

G. Stoclet,*,† R. Séguéla,*,†,§ J. M. Lefebvre,† S. Li,‡ and M. Vert‡

†Université de Lille Nord de France, UMR CNRS 8207, Unité Matériaux Et Transformations, Université Lille 1, Bâtiment C6, 59655 Villeneuve d'Ascq, France

‡Institut de Biomolécules Max Mousseron, UMR CNRS 5247, Faculté de Pharmacie, Université Montpellier 1, 15 Avenue Charles Flahault, 34060 Montpellier, France

ABSTRACT: The present work reports on the study of the influence of the composition in stereomer on the mechanical behavior of D- and L-lactic acid stereocopolymers in relation with strain-induced structural evolution. The stress−strain behavior and structural changes upon stretching above the glass transition temperature have been investigated by means of *in situ* wide-angle X-ray scattering for a series of nearly random stereocopolymers covering a large range of compositions. All members of the family behaved like elastomers in the initial stage of stretching. However, stereocopolymers of low contents in D-units, [D], exhibited a strain-hardening phenomenon starting at strain 150% < ε < 200%, depending on the draw temperature. This strain-hardening decreased with increasing [D] up to the critical concentration [D]* ≈ 8 mol % above which all copolymers displayed an un-cross-linked rubber behavior over the whole strain range. The decrease of the strain-hardening also depended on the draw temperature, yet this sensitivity did not affect the critical concentration [D]* of the position of the transition. The occurrence of the strain-hardening has been correlated with the buildup of a strain-induced ordered phase, the nature of which being directly related to the draw temperature. Drawing at T_d = 90 °C, i.e., about 20−30 °C above T_g depending on the [D] value of the copolymer, resulted in the strain-induced α′-crystalline phase. In contrast, for drawing at $T_d = T_g + 5$ °C, the mesomorphic phase was formed. Moreover, it has been shown that the higher [D], the lower the content of ordered phase, irrespective whether it was crystal or mesophase. A parallel is made between the crystallization capabilities of the copolymers from the quiescent melt and under straining. Only stereocopolymers with [D] < [D]* were able to crystallize from the melt, as in the case of strain-induced crystallization. The occurrence of the strain-induced mesophase only in the case of crystallizable copolymers is taken as a hint of an intermediate state of order precursory to the crystalline state.

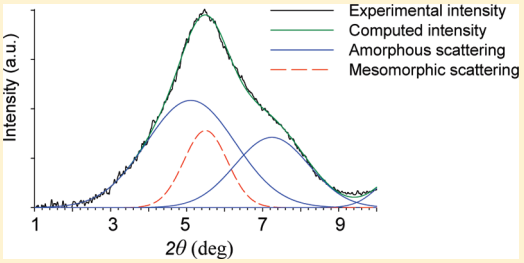

INTRODUCTION

Polymers produced from renewable ressources, especially biomass, have received increasing attention in recent years due to their friendly impact on environment. Lactic acid-based polymers (PLA) are among the most promising candidates for substitution of petroleum-based polymers.[1−6] Indeed, this kind of aliphatic polyester has real potentialities for structural applications owing to fairly good mechanical properties. They were initially developed as sources of devices for biomedical applications in the early 1980s.[7−12] However, some compounded lactic-acid-based polymers also referred to as PLA, essentially semicrystalline ones, have gained interest in various domains like packaging, clothes, etc. relevant to composting.[13]

Poly(lactic acid)s are generally synthesized by ring-opening polymerization of lactides that are dimers of lactic acids. Because of the presence of a chiral center in the lactic acid molecule, there are several lactides, namely L- and D-lactides composed of two L- or two D-lactic acid molecules, respectively; meso lactide composed of one L- and one D-lactic acid molecules, and racemic lactide which is a stoichiometric mixture of L- and D-lactides. Therefore, lactic acid stereocopolymers with different nonbernouillian distribution of chiral repeating units can be synthesized, depending on the composition of the feed in lactides[14]

- Poly(L-lactic acid) and poly(D-lactic acid) are isotactic homopolymers derived from the L-lactide and D-lactide, respectively.
- Racemic poly(lactic acid) is primarily produced from racemic lactide, although a 50/50 L/D stereocopolymer can be also obtained from meso-lactide. However, the resulting two "racemic stereocopolymers have different chiral unit distributions and thus different physical and chemical and structural properties.
- Intermediate stereocopolymers obtained primarily from mixtures of L- and racemic-lactides, although the other lactides can also be used. At the top of the composition in chiral repeating units, their distribution along the chains and the initiator used to polymerized the cyclic dimers are also important factors for structural and material properties.

Received: March 4, 2011
Revised: April 13, 2011
Published: May 20, 2011

- Lactic acid stereocopolymers with bernouillian distribution of the chiral units can be obtained by polycondensation of L- and D-lactic acid although access to high molar mass compounds is still a matter of progress.[15]

From this description of the different synthesis routes and structural particularities, the number of lactic acid stereocopolymers is almost infinite. Therefore, any investigation requires a detailed identification of the PLA used in terms of chirality unit distribution and synthesis conditions to lead to scientifically profitable conclusions. In order to make easier the identification of the various lactic acid stereocopolymers, PLA*X* was introduced as general abbreviation where *X* stands for the percentage of L-units in polymer chains, 100−*X* standing for the content in D-units. Accordingly, the currently used PLLA and PDLLA are PLA100 and PLA50, respectively, PDLA being PLA0.[16]

Although most of the studies reported in the literature have been concerned with the homopolymer PLLA, it has been shown that in the case of PDLLA copolymers, the composition has great influence on the physical properties in relation to the crystallization behavior. From the standpoint of chain microstructure, Chabot et al.[14] have shown that the stereosequence distributions in PLAX copolymers deviated from the expected bernouillian addition of the pairs of units present in lactide molecules. This phenomenon was attributed to trans-esterification during the polymerization, the final distribution being yet not completely random. This behavior was further confirmed by Urayama et al.[17] who showed that, starting from isotactic PLA100, increase of the content in D-isomer resulted in increases of atactic and syndiotactic *diads*. As a consequence, the length of intrachain poly(L-lactic acid) segments sharply decreased with increasing content in D-isomer, with direct changes of the physical properties and crystallization capabilities.

Regarding thermal properties, it has been largely shown that increasing the D-stereomer content resulted in a decrease of the glass transition temperature (T_g) which can span the range 40−60 °C. Moreover it has been shown that the material composition also influenced crystallinity (X_c) and melting temperature (T_m). Indeed, T_m dropped from 190 °C for PLLA down to about 100 °C for PDLLA depending on the content in and the distribution of D-unit.[18−24] In parallel, X_c decreased from 80% down to nil. The decrease of X_c was assigned to the exclusion from the crystalline phase of the stereoregularity defects in the chains that disturb the chain-folding mechanism, a general phenomenon in semicrystalline copolymers that do not display isomorphism.[25] The concomitant shortening of the crystallizable L-isomer segments also entailed a reduction in crystallite thickness that was responsible for the decrease of T_m. This has been given evidence by Runt and co-workers via theoretical analysis of the melting point depression and small-angle X-ray scattering,[20,21] though some inclusion of D-isomer units has been shown to occur under particular crystallization conditions, using NMR spectroscopy.[26,27]

The crystallization kinetics of PLA is also sensitive to composition. The crystallization rates of PLLA (PLA100) and PDLA (PLA0) are rather low, so that amorphous materials can be readily obtained by quenching from the melt, as in the case of poly(ethylene terephthalate) and related copolymers.[28] Introducing D-stereomer units in L-rich chains decreased significantly the crystallization kinetics.[20,21,24,29] This again was assigned to the exclusion from the crystal of the stereoregularity defects that disturbs the mechanism of chain-folding.

Table 1. Molecular and Physical Characteristics of the Various PLA*X* Stereocopolymers

PLA*X* copolymer	*X*	M_n (kDa)	M_w (kDa)	T_g (°C)[a]	T_m[b] (°C)	X_c^{max}[b] (%)
PLA98	98	81	171	60	164	51
PLA96	96	114	225	60	152	47
PLA94	94	109	211	59	142	42
PLA92	92	95	180	57	135	36
PLA75	75	103	205	55	-	0
PLA62	62	81	170	53	-	0
PLA50	50	76	180	52	-	0

[a] Glass transition temperature from the DSC heating scans of the amorphous compression molded samples. [b] Peak melting temperature and maximum crystallinity from the DSC heating scans of samples isothermally crystallized for 2 h at 120 °C.

Although numerous studies have been concerned with the thermal crystallization of PLLA and PDLLA,[18−24,29−37] very few studies have addressed the question of strain-induced crystallization.[38−44] Former works regarding the crystallography of PLLA were carried out on drawn fibers[45−49] without particular attention to the mechanism of the process. In a study regarding the crystallization upon stretching of a PLA having [D] = 2 mol %, Mulligan and Cakmak[39] claimed for the buildup of a strain-induced nematic order as judged from the appearance of a strong equatorial scattering. Mahendrasingam et al.[40] also reported the occurrence of a disordered crystal form for draw temperatures below 100 °C, for a PLA having [D] = 4 mol %. The influence of composition on strain-induced crystallization capabilities has not been investigated yet, though this aspect is of prime interest in view of controlling the final structure of the material after processing.

In previous papers,[43,44] we reported that the degree of strain-induced ordering of a commercial PLA containing [D] = 4.3 mol % was dependent on the draw conditions. Especially, a mesophase was generated when drawing was performed at temperatures below or slightly above T_g whereas the α′-crystalline phase grew up for draw temperatures well above T_g. The mesophase was clearly identified by its X-ray scattering pattern which exhibits a characteristic peak twice as large as the crystalline peaks but much narrower than the amorphous halo.[43] Mulligan and Cakmak more precisely claimed for a nematic order,[39] whereas a *condis crystal* may also be suspected.[43] The occurrence of the mesophase has been interpreted in terms of chain dynamics in relation to draw temperature and strain rate.,[39,43] Similar kind of mesophase was recently given evidence via spectroscopic techniques in PLA-based materials after either stretching[50] or thermal treatment about T_g.[51,52] These conformational data vouch in favor of the *condis crystal* hypothesis.

The present paper reports on the investigation of the quiescent crystallization of a series of PLAX stereocopolymers covering a large range of X values, and on the *in situ* study of the strain-induced ordering upon uniaxial stretching above T_g. Comparisons are made between quiescent and strain-induced crystallization capabilities.

EXPERIMENTAL SECTION

Material and Preparation. The PLAX stereocopolymers used in this study were synthesized by ring-opening polymerization of suitable

mixtures of L-lactide and racemic-lactide. More details regarding the synthesis are given elsewhere.[14] Table 1 summarizes the main characteristics of the various members of the family. The number-average, M_n, and weight-average, M_w, molar masses of the copolymers were determined by size exclusion chromatography. Their composition was assessed from nuclear magnetic resonance which also revealed that the distribution of L- and D-chiral lactate units was preferentially isotactic, i.e., not random in terms of Bernouillian statistics.

The stereocopolymers were rapidly compression-molded into ~500 μm thick sheets at 180 °C in a hot press. The sheets were rapidly cooled down to room temperature (RT) by air convection in order to quench the copolymers in the amorphous state.

Differential Scanning Calorimetry (DSC). Thermal analysis was carried out using a Perkin-Elmer DSC7. The apparatus was calibrated using standard procedures with a high purity indium sample. All heating scans were recorded at a heating rate of 10 °C/min. Isothermal crystallization was investigated at two temperatures T_{cr} = 90 °C and T_{cr} = 120 °C. The samples weighting 5−8 mg were held in the melt at 180 °C for 5 min, before cooling at 40 °C/min to the given isothermal temperature. The melting point, T_m, was determined at the peak of the melting endotherm and the glass transition temperature, T_g, was assessed from the inflection point of the heat capacity jump. The crystalline weight fraction, X_c, was computed from the enthalpy of the melting endotherm using the specific enthalpy of fusion of the perfect crystal $\Delta H_f^\circ \approx 94$ J/g after Fischer et al.[26]

Tensile Drawing. For the *in situ* WAXS study of the strain-induced structural changes, a homemade tensile testing stage allowing symmetrical drawing of the samples was used. Parallelepipedic test pieces 4 mm in gauge length and 3 mm wide were cut off the 500 μm thick sheets. The crosshead speed was 2.4 mm/min that corresponded to an initial strain rate $\dot{\varepsilon} = 0.01\ s^{-1}$. The nominal strain is defined as $\varepsilon_N = L/L_o$, where L and L_o are the gauge lengths of the sample during and prior to deformation, respectively. The nominal stress $\sigma_N = F/S_o$ is computed from the applied force, F, and the initial sample cross-section area, S_o. Considering that all materials deformed in a roughly homogeneous way above T_g, the nominal strain, ε_N, was very close to the actual local strain, ε, and the true stress, σ_T, can be computed as $\sigma_T = \sigma_N(1 + \varepsilon)$.

Wide-Angle X-ray Scattering (WAXS). *In situ* WAXS measurements during drawing were carried out on the BM02 beamline at the European Synchrotron Radiation Facility (Grenoble, France) using an X-ray energy of 24 keV, i.e., λ = 0.51 Å. The point-focused beam was 300 μm in diameter. The through-view 2D-patterns were recorded using a CCD camera from Princeton Instruments, the acquisition time being 5 s every 7 s. Corrections were applied for background scattering, geometry and intensity distortions of the detector. Both incoming and transmitted intensities were measured synchronously with WAXS data acquisition. Thereby the transmission factor, defined as the ratio between the transmitted intensity and the incident intensity, was calculated and used to normalize the integrated intensity profiles.

Static WAXS experiments were also carried out at RT for characterizing the crystalline structure of isotropic samples as a function of thermal treatment using a Genix microsource from Xenocs operated at 50 kV and 1 mA. The Cu−Kα radiation (λ = 1.54 Å) was collimated with a FOX2D mirror and two pairs of Scatterless slits from Xenocs. The 2D-patterns were recorded on a CCD camera from Photonic Science.

Radial intensity profiles, $I(2\theta)$, were obtained by azimuthal integration of the 2D-patterns over 180° by means of the *FIT2D* software. Quantitative assessment of the weight fractions of the amorphous, mesomorphic and crystalline phases, X_{am}, X_{meso}, and X_c, respectively, were made thanks to a previously described method[43] using the PeakFit software, and assuming Gaussian profiles for all scattering peaks and amorphous halos. The amorphous intensity profile was experimentally identified to the scattering pattern of the thoroughly amorphous undrawn sample, regarding both position and full width at half-maximum (fwhm).

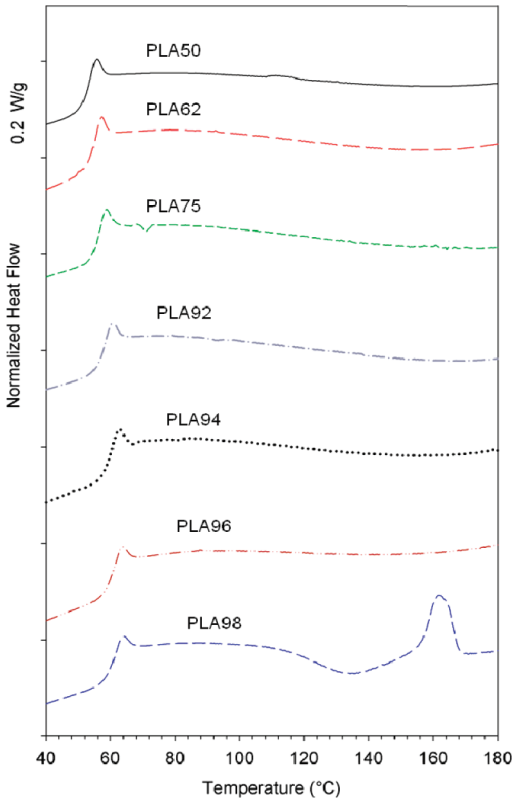

Figure 1. DSC heating scans of the compression-molded copolymer sheets.

The strain-induced crystalline α′ form was clearly identified at T_d > 80 °C by sharp peaks having fixed angular position: only the fwhm and intensity were allowed to self-adjust during the PeakFit treatment of all WAXS profiles. Samples drawn at T_d < 80 °C, i.e., just above the glass transition temperature, made it possible to identify the contribution of the mesomorphic form in the absence of crystal scattering, as described in the previous studies.[43,44]

RESULTS

Crystallization and Melting of Isotropic Samples. Prior to investigate the tensile drawing behavior of the copolymers and the strain-induced structural changes, it was mandatory to characterize the quiescent crystallization capabilities of these copolymers. Figure 1 reports the DSC heating traces of the compression-molded sheets. Except PLA98 that displays a faint crystallization exotherm and a subsequently melting endotherm, most copolymers only display a glass transition heat capacity jump indicative of thoroughly amorphous materials. The T_g follows a rather common monotonic decreasing with increasing [D], as can be also seen from the data of Table 1. The lower amplitude of the T_g drop as compared with Urayama et al.'s data[17] is probably due to the fact that the distributions of the D-units in the present stereocopolymers was different probably because of different polymerization conditions, especially initiator and catalyst.

The DSC traces of isothermally crystallized samples for 2 h at 120 °C are reported in Figure 2. The clear-cut melting endotherm for copolymers PLA98, PLA6, PLA94, and PLA92 indicates that all four were semicrystalline. This means that these copolymers were actually quenched in the amorphous state upon

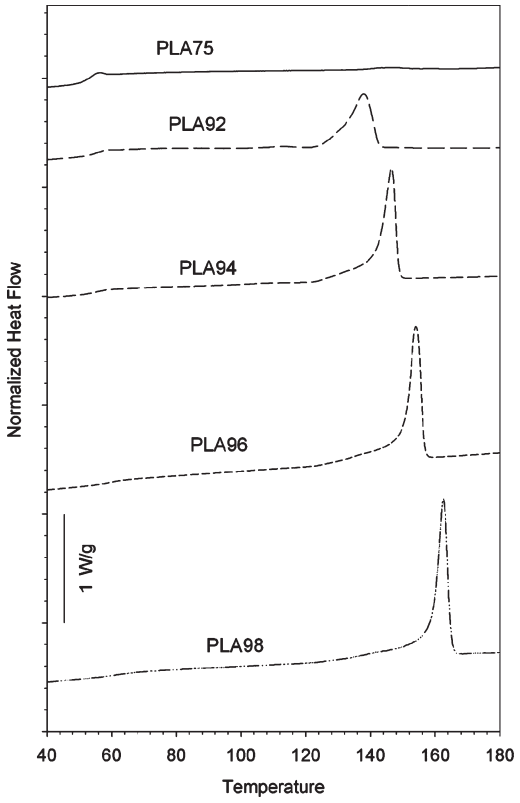

Figure 2. DSC heating scans of the copolymers isothermally crystallized for 2 h at 120 °C.

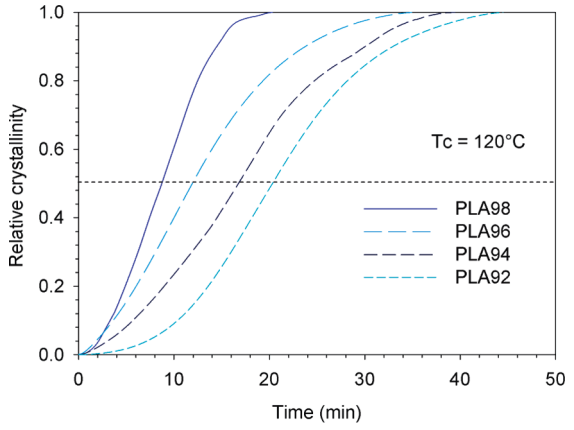

Figure 3. Crystal conversion as a function of time for isothermal crystallization of the copolymers at 120 °C.

compression-molding. Besides, their inability (or at least weak ability concerning PLA98) to crystallize during the heating scan at 10 °C/min from the amorphous state (Figure 1) suggested rather low crystallization rates. In contrast, copolymers PLA75, PLA62, and PLA50 did not display any hint of melting (Figure 2), even after 8 h of isothermal crystallization at 120 °C. This is a piece of evidence that these copolymers have no crystallization potentiality at all, at previously reported.[7,8]

Further investigation of the thermal behavior of the copolymers has been performed via analysis of the isothermal crystallization kinetics. Figure 3 shows the relative crystal content as a function of time for the crystallization temperature T_{cr} = 120 °C.

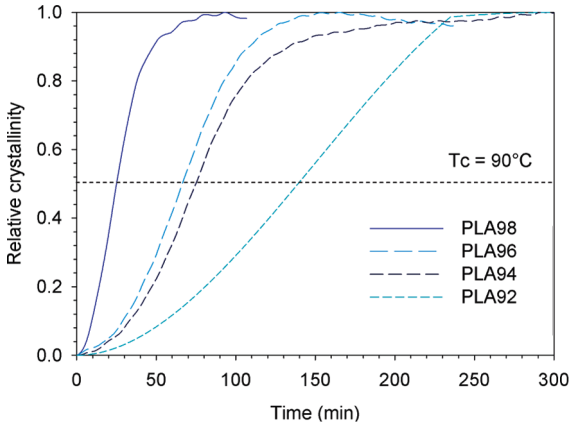

Figure 4. Crystal conversion as a function of time for isothermal crystallization of the copolymers at 90 °C.

The crystallization kinetics strongly slowed down when [D] increased. Indeed, the crystallization half-time increased from 8 min for PLA98 to about 20 min for PLA92. In parallel, completion of crystallization took 20 min for PLA98 and about 45 min for PLA92. This trend is similar to that reported by Cho et al.[53] from *in situ* WAXS data on three copolymers presented as random. Moreover, copolymers with [D] > 8% appear to be thoroughly amorphous after isothermal treatment for up to 4 h, indicating total inability for crystallization. This latter finding is consistent with Urayama et al.'s observations,[17] but drastically deviates from Sarasua et al.'s data[22] due to strong difference in L/D distributions of the copolymers in addition to lower molar weight that may hasten crystallization.[31,54] The latter copolymers contain stereoblocs that generate a stereocomplex crystallization whatever the [D] value.[22]

In order to confirm these findings, isothermal crystallizations were also conducted at T_{cr} = 90 °C, a temperature which was roughly in the midrange of temperature between glass transition and melting of the potentially crystallizable copolymers. Figure 4 shows the relative crystal content as a function of time. The crystallization rate was drastically reduced as compared with T_{cr} = 120 °C, yet similar trend is observed for the various copolymers: the higher the [D] value, the lower the crystallization rate. Moreover, copolymers with [D] > 8% remain thoroughly amorphous even after 8 h of isothermal crystallization.

The T_m and X_c^{max} data of samples isothermally crystallized for 2 h at T_{cr} = 120 °C are reported in Table 1. The T_m drop with increasing [D] suggests an increase of crystallographic defects and/or reduction of crystal thickness. Besides, the abruptness of this drop indicates that very low [D] values have a dramatic effect, in agreement with Grijpma and Pennings' observation.[18] The X_c^{max} data reveal that the stereodefects are responsible for a loss of crystallinity of the copolymers down to nil when [D] > 8%. This finding supports the hypothesis that these structural chain defects are rejected out of the crystalline phase, since isomorphism generally lead to very gradual loss of crystallinity in copolymers.[25]

The evolution of the shape of the melting endotherm is also informative regarding the structural habits of the copolymers in the isotropic state. The DSC heating traces of the crystallizable copolymers after isothermal crystallization at T_{cr} = 120 °C for 2 h (Figure 2) exhibit a unique melting endotherm relevant to a rather stable crystalline structure that does not undergo reorganization during the heating scan. The WAXS intensity profiles

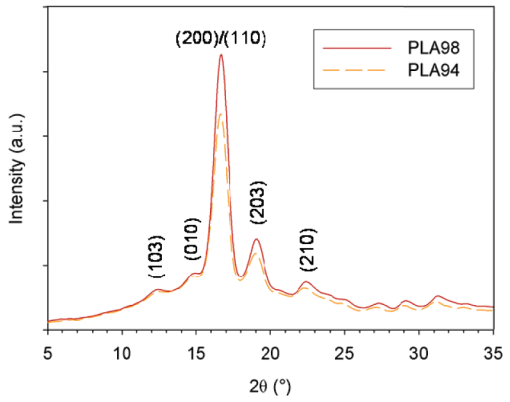

Figure 5. WAXS intensity profiles recorded at RT of PLA98 and PLA94 isothermally crystallized for 2 h at 120 °C (X-ray wavelength λ = 1.54 Å).

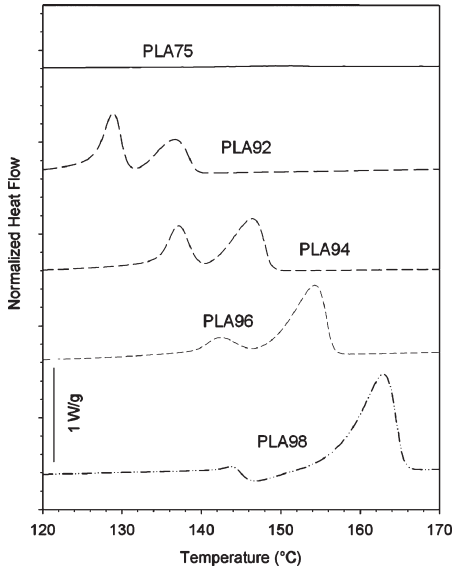

Figure 6. DSC melting endotherms the copolymers after isothermal crystallization for 4 h at 90 °C.

reported in Figure 5, for these samples prior to the DSC heating scan, reveal that the crystals were initially in the stable pseudo-orthorhombic α form, as deduced from the presence of the minor reflections (103), (010), and (210) in addition to the main scattering peaks (200)/(110) and (203).[55] Moreover, the similar width at half-height of the above-mentioned peaks for both PLA98 and PLA94 indicates that the mosaic block size in the lamellar crystals is the same in the two copolymers and does not depend on the [D] value. This supports the previous hypothesis that the stereodefects are in majority rejected from the crystalline phase.

In contrast, for the isothermal crystallization for 4 h at T_{cr} = 90 °C, the DSC heating traces of Figure 6 show a double melting peak indicative of an unstable crystalline structure that reorganizes during the heating scan, as already reported in literature in the case of PLLA.[56−58] The WAXS patterns of Figure 7 give clear evidence that these samples were predominantly in the defective α′ crystal form prior to the DSC heating scan, as judged from the missing of the minor reflections and the very slight shift to low scattering angle of the two major peaks (see Figure 5). This is consistent with Zhang et al. regarding the

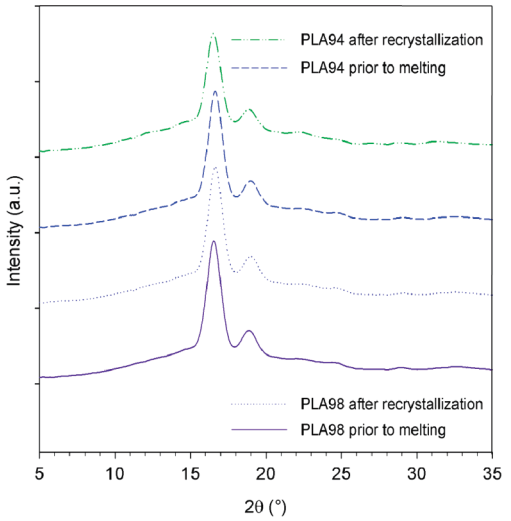

Figure 7. WAXS intensity profiles recorded at RT of PLA98 and PLA94 isothermally crystallized for 4 h at 90 °C: prior to melting and after melting-recrystallization (X-ray wavelength λ = 1.54 Å).

isothermal crystallization of PLLA below 120 °C.[55] Surprisingly, after recrystallization above 120 °C during the heating scan, all crystallizable copolymers are still in the α′ crystal form. This means that recrystallization did not allow the more perfect α crystals to grow during the heating scan at 10 °C/min, in contrast to long duration isothermal crystallization at 120 °C. This is yet consistent Zhang et al.[55] who showed that the α−α′ transition upon heating at 2 °C/min starts at 150 °C only.

A striking feature of the double melting peaks (Figure 6) is that the area of the low T_m peak increased in parallel to [D], in spite of the gradual loss of crystallinity. The most probable origin to this phenomenon is the slowing down of the crystallization kinetics with increasing [D] that entailed a reduced amount of recrystallized material for the same laps of time at the same heating rate. Thus, the energy balance between crystal melting and recrystallization increasingly turned favorable to the former process. The increasing depletion of the high T_m peak area thoroughly supports the hypothesis of reduced recrystallization capabilities.

The crystallization exotherm, which appeared only for PLA98 (Figure 6), suggested that the melting-crystallization is unbalanced in favor of the second process for this copolymer, i.e. a greater content of new crystals was generated after melting of the initial ones. The absence of crystallization exotherm between the two melting peaks for the other copolymers means that not all the initial crystals were able to recrystallize after melting. This may be assigned to the decreasing gap between of the two successive melting peaks that reduces the recrystallization ability of the copolymers with increasing [D]. This is consistent with the previous argumentation regarding the opposite evolution of the low T_m and high T_m peak areas.

It is surprising that all crystallizable copolymers were able to generate α crystals, in spite of chains defects, particularly regarding PLA92. This finding vouches in favor of exclusion of the D-isomer units from the crystal, allowing thus only pure L-sequences to be involved in the crystallization process.[20,21] Indeed, in this instance, nothing prevents the growth crystals in the most ordered α form, as far as crystallization takes place at a temperature above that of the well-known α′−α transition,

i.e., about 110 °C.[35,55] This is precisely the case for the recrystallization of the samples isothermally crystallized at 90 °C (Figure 6).

In Situ WAXS Analysis of Tensile Drawing. It is worth noticing first that crystallinity is about nil or very weak for any of the crystallizable copolymers for isothermal crystallization time shorter than 15 min, which is the time scale of the drawing tests. Therefore, minor thermal crystallization was expected during the mechanical tests at T_d = 90 °C, and below this temperature. Figure 8 shows the stress−strain curves of PLAX at T_d = 90 °C, i.e., well above T_g. All PLAX behaved like un-cross-linked rubbers until $\varepsilon \approx 200\%$, whatever [D]. Beyond this strain threshold, two situations appeared. Copolymers with [D] ≤ 8% exhibited a strain-hardening phenomenon, the lower [D] the higher the slope of this strain-hardening. For [D] > 8%, no strain-hardening phenomenon was observed so that the polymers still behave like un-cross-linked rubbers for ε > 200%.

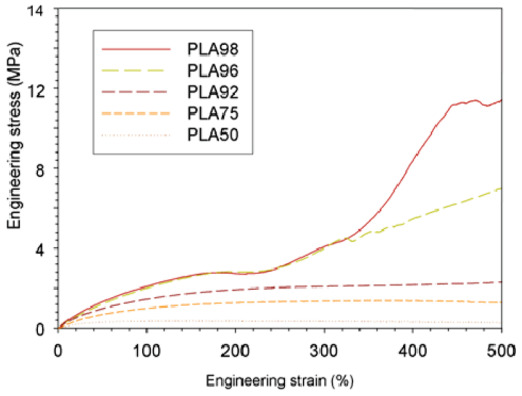

Figure 8. Engineering stress−strain curves of copolymers drawn at T_d = 90 °C.

As previously reported for a PLA with [D] = 4.3%,[44] for similar draw conditions, one may expect the strain-induced hardening to result from a molecular ordering. Parts a and b of Figure 9 show the 2D-WAXS patterns of PLA98 and PLA50 strained at T_d = 90 °C up to ε = 400%. The sharp diffraction arcs of PLA98 revealed a true strain-induced crystallization with well oriented crystals having their (hk0) planes parallel to the draw axis. In contrast, a diffuse and slightly anisotropic halo appeared for PLA50. This means that crystallization did occur during drawing, and that chain relaxation has been active in the meantime in spite of high elongation. Thus, the missing of strain-induced crystallization for PLA50 resulted from its inability to build up crystalline order, as already observed in the case of quiescent crystallization.

Azimuth-integrated intensity profiles from the 2D-patterns of PLA98 and PLA50 are reported in Figure 9, parts c and d,

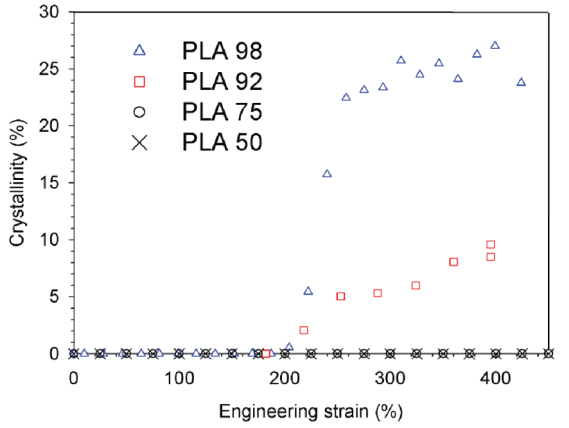

Figure 10. *In situ* crystal content versus of strain for the drawing of the copolymers at T_d = 90 °C.

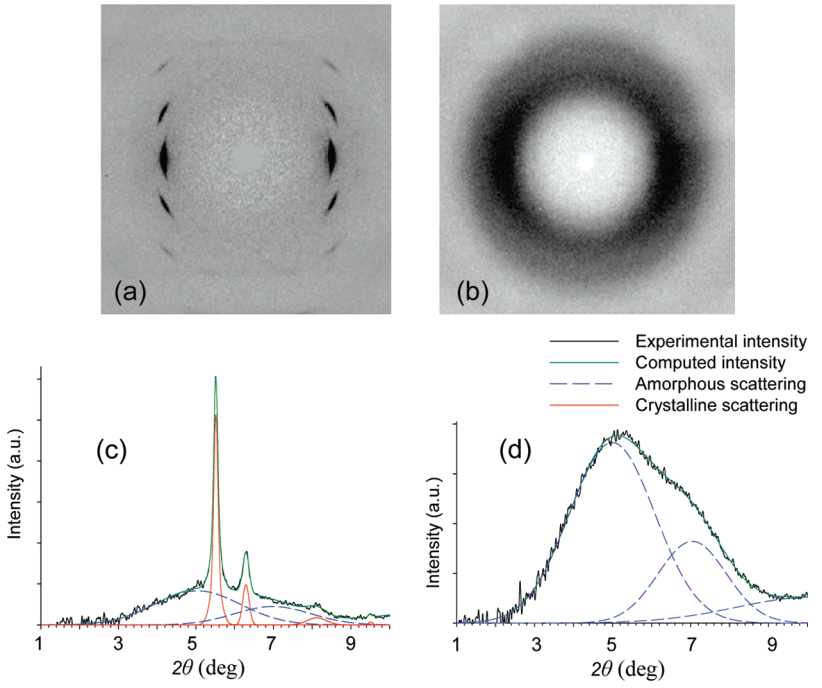

Figure 9. *In situ* 2D-WAXS patterns of (a) PLA98 and (b) PLA50 copolymers drawn $\varepsilon_N \approx 400\%$ at T_d = 90 °C; azimuth-integrated intensity profiles of the 2D-patterns of (c) PLA98 and (d) PLA50 together with curve fitting analysis (X-ray wavelength λ = 0.51 Å).

dx.doi.org/10.1021/ma200469t |*Macromolecules* 2011, 44, 4961–4969

respectively. In the case of PLA98, the diffraction peak positions indicate that the strain-induced crystalline phase is of the α′ form.[35,55] Regarding PLA50, the intensity profile is quite similar to the one of the undrawn amorphous sample, confirming that absolutely no crystallization occurred during drawing.

Using the peak deconvolution method described in the previous studies,[43,44] the structural evolution with strain of the stereocopolymers has been quantitatively determined. The data of Figure 10 show that for polymers with [D] ≤ 8%, the strain-induced crystallization process started at $\varepsilon \approx 200\%$ and leveled off quickly. The sigmoid shape of the X_c versus ε curve was roughly the same for the various copolymers, and similar to previous observation.[44] This means that there is a threshold of strain and/or chain orientation for promoting crystallization. It also appears that $X_c^{max} \approx 25\%$ for PLA98 at high strains, whereas $X_c^{max} \approx 5\%$ for PLA92. In other words, the higher the [D] value, the lower X_c^{max}. Moreover, Figure 10 clearly shows that strain-induced crystallization no longer occurred for PLA75 and PLA50 whatever the draw ratio. These findings will be further discussed in the next section.

It appears from Figure 10 that in spite of various maximum crystallinity, the crystallizable copolymers exhibit very similar kinetics of strain-induced crystallization. This emphasizes the predominant role of chain orientation over that of chain mobility on the ordering process. It is also worth noticing that the strain-induced X_c^{max} value of every copolymer is somewhat lower than in the case of isothermal crystallization (Table1). This is due to the fact that strain-induced crystallization was not optimized with regard to both temperature and strain rate.

A second draw temperature $T_d = T_g + 5$ °C has been considered in order to investigate the capability of the present copolymers to develop a strain-induced mesophase, as previously observed in the case of a commercial PLA.[43,44] The stress−strain curves of the copolymers are reported in Figure 11. All materials exhibited a rubber-like behavior for strains $\varepsilon < 150\%$, owing to the low strain rate strain rate = 0.01 s^{-1}. Beyond this strain, two situations occur:

- For [D] ≤ 8%, a strain-hardening phenomenon occurred, the slope of which decreased with increasing [D] value.
- For [D] > 8%, the materials still behaved like un-cross-linked rubbers without strain-hardening up to rupture.

Parts a and b of Figure 12 report the 2D-WAXS patterns of copolymers PLA98 and PLA50 drawn up to $\varepsilon = 400\%$ at $T_d = T_g + 5$ °C. No trace of crystal reflections appears in each case. Chain orientation parallel to the draw direction is well developed for PLA98 whereas PLA50 was only slightly oriented. Analysis of the azimuth-integrated intensity profiles of Figure 12, parts c and d revealed that, at $\varepsilon = 400\%$, PLA98 contained a large amount of mesophase whereas PLA50 appeared thoroughly amorphous. Obviously, the strain-induced generation of the cohesive

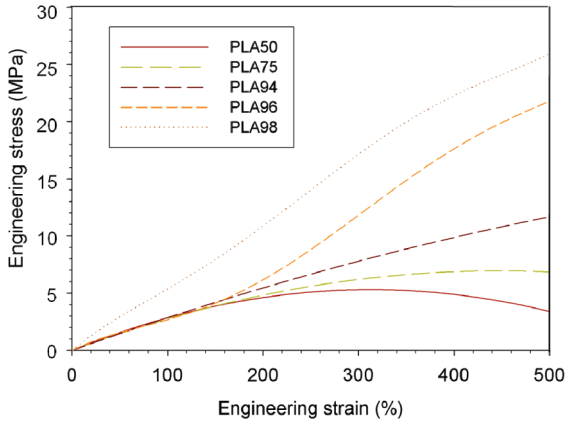

Figure 11. Engineering stress−strain curves of copolymers drawn at $T_d = T_g + 5$ °C.

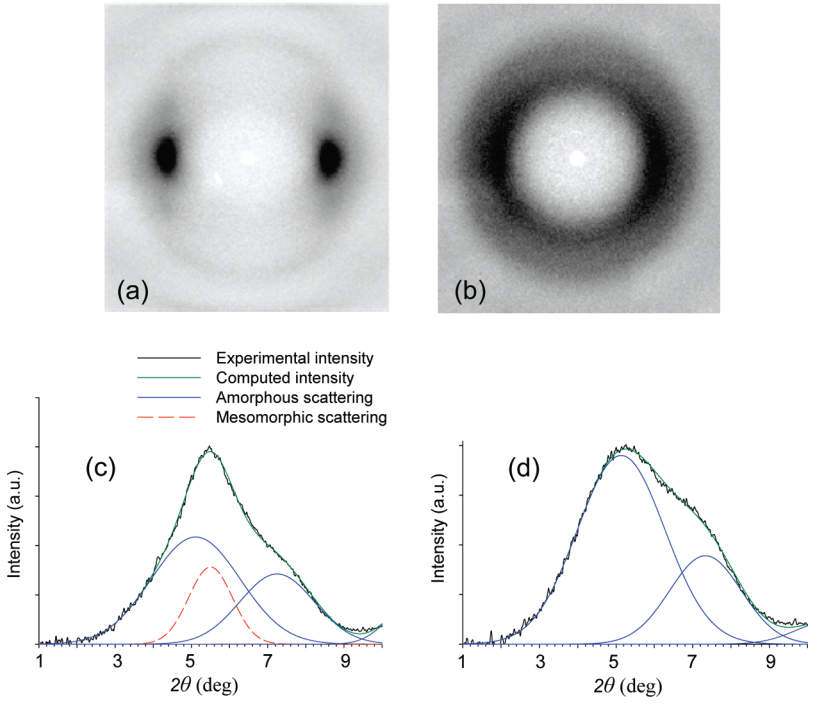

Figure 12. *In situ* 2D-WAXS patterns of (a) PLA98 and (b) PLA50 copolymers drawn $\varepsilon_N \approx 550\%$ at $T_d = T_g + 5$ °C; azimuth-integrated intensity profiles of the 2D-patterns of (c) PLA98 and (d) PLA50 together with curve fitting analysis (X-ray wavelength $\lambda = 0.51$ Å).

dx.doi.org/10.1021/ma200469t |*Macromolecules* 2011, 44, 4961–4969

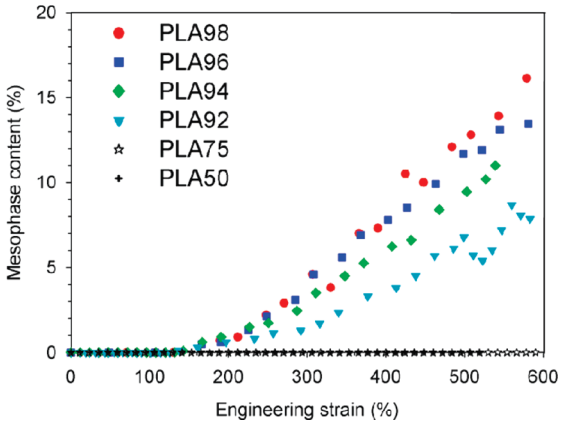

Figure 13. *In situ* mesophase content as a function of strain for the drawing of the copolymers at $T_d = T_g + 5$ °C.

mesophase preserved the strain-induced chain orientation in PLA98, whereas the absence of strain-induced cohesive phase allowed chain relaxation during drawing of PLA50.

By deconvolution of the intensity profiles, using the previously described method, the amount of strain-induced mesophase was calculated as a function of strain for every material. The results reported in Figure 13 indicated that beyond $\varepsilon \approx 150\%$, X_{meso} increases almost linearly with increasing strain. Moreover it appears that, at a given strain, the higher the [D] value, the lower the mesophase content. The maximum content in mesophase for the present stereocopolymers dropped from $X_{meso}^{max} \approx 18\%$ for PLA98 down to $X_{meso}^{max} \approx 8\%$ for PLA92. For copolymers having [D] > 8%, no mesophase is observed, in a similar way as no crystalline phase occurred for $T_d = 90$ °C.

CONCLUDING DISCUSSION

This work shows that the strain-induced structural evolution and the mechanical behavior of the studied lactic acid stereocopolymers strongly depended on both composition in stereomers and draw temperature.

Regarding the temperature, drawing at $T_d = 90$ °C, i.e. 20−30 °C above T_g, generated a α′-crystalline phase. Drawing at $T_d = T_g + 5$ °C generated a mesomorphic phase. However, a common tendency appears for the two temperatures. The copolymers that were prone to strain-induced crystallization were also those able to generate a mesophase. Moreover, the higher the level of strain-induced crystallization, the higher the limiting content of mesophase. These findings suggest that a structural correlation existed between crystal and mesophase; i.e., the mesophase could be a precursor of the crystalline state of PLA. The dual distribution of oriented Keesom forces between the polar ester groups and dispersive London forces between nonpolar methyl groups that governs the buildup of the helical conformation of PLA[45] may be the driving force for stepwise packing during the strain-induced chain ordering. This hypothesis is supported by Na et al.[59] who recently suggested occurrence of a sequential ordering process during cold-crystallization of PLLA, in terms of conformational arrangements. The actual mechanism of ordering is still unknown. However, it is well-known that chain dynamics have to be taken into consideration since chain relaxation operates against chain orientation.[39,44] This phenomenon directly influence the mechanisms of chain ordering and therefore modifies the occurrence of either mesophase or crystal depending on draw temperature and strain rate.

The mechanical consequence of the strain-induced ordering is strain-hardening, in the case of the crystalline phase, and of the mesophase as well. This strain-hardening effect is particularly remarkable regarding the mesophase. It corroborates the previous conclusion that the mesophase is nearly as much cohesive as the crystalline phase in spite of its partial disorder.[44]

The ability for strain-induced crystallization and mesophase formation directly connected with the capability of the copolymers to crystallize from the quiescent melt. There is a critical D-isomer content $[D]^* \approx 8\%$ above which no crystallization is possible, via either thermal or mechanical means. This critical $[D]^*$ value is close to data reported in the literature regarding thermal crystallization of nearly random copolymers.[17−19] It is suggested that beyond this value the length of the L-isomer sequences is too small for occurrence of chain-folding crystallization, in the assumption that the D-units are excluded from the crystalline phase.

Copolymers unable to crystallize displayed the typical mechanical behavior of an un-cross-linked rubbery network. In the meantime that stretching induced an alignment of the chains along the draw direction, the relaxation processes and entropic back stress allowed the oriented chains to fold back to nearly random conformation.

Worth noticing is the difference between thermal and strain-induced crystallization in terms of kinetics. The increase of [D] resulted in a severe slowing down of isothermal crystallization. In contrast, the kinetics of strain-induced crystallization proved to be insensitive to the D-isomer content. In this instance, only the maximum crystal content was sensitive to the copolymer composition. This points out the major role of chain orientation over that of temperature-governed chain mobility on the activation of the crystallization process. Molecular mobility is yet involved in the level or order that can be reached during stretching, i.e., crystal versus mesophase, as pointed out in one of the previous studies.[44]

AUTHOR INFORMATION

Corresponding Author

*E-mail: (G.S.) gregory.stoclet@univ-lille1.fr; (R.S.) roland.seguela@insa-lyon.fr.

Present Addresses

[§]MATEIS, Bat. Blaise Pascal, INSA de Lyon, 69621 Villeurbanne, France.

ACKNOWLEDGMENT

The European Synchrotron Radiation Facility (ESRF, Grenoble, France) is gratefully acknowledged for beamtime allocation on the BM02 line. Dr. Cyrille Rochas is also acknowledged for assistance in the experiments at ESRF. The authors are indebted to the Region Nord/Pas-de-Calais and the European FEDER program for funding to the X-ray equipment at UMET.

REFERENCES

(1) Sinclair, R. G. *J. Macromol. Sci.—Pure Appl. Chem.* **1996**, *33* 585–597.

(2) Sodergard, A.; Stolt, M. *Prog. Polym. Sci.* **2002**, *27*, 1123–1163.

(3) Auras, R. A.; Harte, B.; Selke, S. *Macromol. Biosci.* **2004**, *4*, 835–864.
(4) Averous, L. In *Monomers, Polymers and composites from renewable resources*; Belgacem, M. N., Gandini, A., Eds.; Elsevier Ltd.: Oxford, U.K.; 2008; pp 433−450.
(5) Williams, C. K.; Hillmyer, M. A. *Polym. Rev.* **2008**, *48*, 1–10.
(6) Nampoothiri, K. M.; Nair, N. R.; John, R. P. *Bioresour. Technol.* **2010**, *101*, 8493–8501.
(7) Vert, M.; Chabot, F.; Leray, J.; Christel, P. *Makromol. Chem.* **1981**, No. Suppl. 5, 30–41.
(8) Vert, M.; Christel, P.; Chabot, F.; Leray, J. In *Macromolecular Biomaterials*; Hastings, G. W., Ducheyne, P., Eds.; CRC Press Inc.: New York; 1984; pp 119−141.
(9) Rokkanen, P. U.; Bostman, O.; Hirvensalo, E.; Makela, E. A.; Partio, E. K.; Patiala, H.; Vainionpaa, S.; Vihtonen, K.; Tormala, P. *Biomaterials* **2000**, *21*, 2607–2613.
(10) Pandey, R.; Khuller, G. K. *Curr. Drug Deliv.* **2004**, *1*, 195–201.
(11) Garvin, K.; Feschuk, C. *Clin. Orthop. Rel. Res.* **2005**, *437*, 105–10.
(12) Tokiwa, Y.; Calabia, B. P. *Appl. Microbiol. Biotechnol.* **2006**, *72* 244–251.
(13) Vink, E. T. H.; Rabago, K. R.; Glassner, D. A.; Springs, B.; O'Connor, R. P.; Kolstad, J.; Gruber, P. R. *Macromol. Biosci.* **2004**, *4*, 551–564.
(14) Chabot, F.; Vert, M.; Chapelle, S.; Granger, P. *Polymer* **1983**, *24*, 53–59.
(15) Moon, S. I.; Kimura, Y. *Polym. Intern.* **2003**, *52*, 299–303.
(16) Vert, M. In *Biopolymers—Polyesters III: Applications and Commercial Products*; Steinbüchel, A., Doi, Y., Eds.; Wiley VCH: Weinheim, Germany; 2002; Vol. 4, p179−202.
(17) Urayama, H.; Kanamori, T.; Kimura, Y. *Macromol. Mater. Eng.* **2001**, *286*, 705–713.
(18) Grijpma, D. W.; Pennings, A. J. *Macromol. Chem. Phys.* **1994**, *195*, 1633–47.
(19) Tsuji, H.; Ikada, Y. *Macromol. Chem. Phys.* **1996**, *197*, 3483–3499.
(20) Huang, J.; Lisowski, M. S.; Runt, J.; Hall, E. S.; Kean, R. T.; Buehler, N.; Lin, J. S. *Macromolecules* **1998**, *31*, 2593–2599.
(21) Baratian, S.; Hall, E. S.; Lin, J. S. R.; Runt, J. *Macromolecules* **2001**, *34*, 4857–4864.
(22) Sarasua, J.-R.; Prud'homme, R. E.; Wisniewski, M.; Le Borgne, A.; Spassky, N. *Macromolecules* **1998**, *31*, 3895–3905.
(23) Sodergard, A.; Stolt, M. *Prog. Polym. Sci.* **2002**, *27*, 1123–1163.
(24) Abe, H.; Harigaya, M.; Kikkawa, Y.; Tsuge, T.; Doi, Y. *Biomacromolecules* **2005**, *6*, 457–467.
(25) Wunderlich, B. *Macromolecular Physics, Vol. 1: Crystal Structure, Morphology, Defects*; Academic Press: New York ; 1973; Chapter 2.
(26) Fischer, E. W.; Sterzel, H. J.; Wegner, G. *Kolloid Z. Z. Polym.* **1973**, *251*, 980–990.
(27) Zell, M. T.; Padden, B. E.; Paterick, A. J.; Hillmyer, M. A.; Kean, R. T.; Thakur, K. A. M.; Munson, E. J. *J. Am. Chem. Soc.* **1998**, *120*, 12672–12673.
(28) Kint, D. P. R.; Munoz-Guerra, S. *Polym. Int.* **2003**, *52*, 321–336.
(29) Liu, Y.; Wang, L.; He, Y.; Fan, Z.; Li, S. *Polym. Int.* **2010**, *59*, 1616–1621.
(30) Tsuji, H.; Ikada, Y. *Polymer* **1995**, *36*, 2709–16.
(31) Abe, H.; Kikkawa, Y.; Inoue, Y.; Doi, Y. *Biomacromolecules* **2001** *2*, 1007–1014.
(32) Pluta, M.; Galeski, A. *J. Appl. Polym. Sci.* **2002**, *86*, 1386–1395.
(33) Kulinski, Z.; Piorkowska, E. *Polymer* **2005**, *46*, 10290–10300.
(34) Tsuji, H.; Takai, H.; Saha, S. K. *Polymer* **2006**, *47*, 3826–3837.
(35) Yasuniwa, M.; Tsubakihara, S.; Iura, K.; Ono, Y.; Dan, Y.; Takahashi, K. *Polymer* **2006**, *47*, 7554–7563.
(36) Masirek, R.; Piorkowska, E.; Galeski, A.; Mucha, M. *J. Appl. Polym. Sci.* **2007**, *105*, 282–290.
(37) Pan, P.; Liang, Z.; Zhu, B.; Dong, T.; Inoue, Y. *Macromolecules* **2008**, *41*, 8011–8019.
(38) Kokturk, G.; Serahtkulu, T. F.; Cakmak, M.; Piskin, E. *Polym. Eng. Sci.* **2002**, *42*, 1619–1628.
(39) Mulligan, J.; Cakmak, M. *Macromolecules* **2005**, *38*, 2333–2344.
(40) Mahendrasingam, A.; Blundell, D. J.; Parton, M.; Wright, A. K.; Rasburn, J.; Narayanan, T.; Fuller, W. *Polymer* **2005**, *46*, 6009–6015.
(41) Ghosh, S.; Vasanthan, N. *J. Appl. Polym. Sci.* **2006**, *101*, 1210–1216.
(42) Pluta, M.; Galeski, A. *Biomacromolecules* **2007**, *8*, 1836–1843.
(43) Stoclet, G.; Seguela, R.; Lefebvre, J.-M.; Elkoun, S.; Vanmansart, C. *Macromolecules* **2010**, *43*, 1488–1498.
(44) Stoclet, G.; Seguela, R.; Lefebvre, J.-M.; Rochas, C. *Macromolecules* **2010**, *43*, 7228–7237.
(45) De Sanctis, P.; Kovacs, A. J. *Biopolymers* **1968**, *6*, 299–306.
(46) Eling, B.; Gogolewski, S.; Pennings, A. J. *Polymer* **1982**, *23*, 1587–1593.
(47) Hoogsteen, W.; Postmena, A. R.; Pennings, A. J.; Ten Brinke, G.; Zugenmaier, P. *Macromolecules* **1990**, *23*, 634–642.
(48) Sawai, D.; Takahashi, K.; Sasashinge, A.; Kanamoto, T.; Hyon, S. H. *Macromolecules* **2003**, *36*, 3601–3605.
(49) Takahashi, K.; Sawai, D.; Yokoyama, T.; Kanamoto, T.; Hyon, S. H. *Polymer* **2004**, *45*, 4969–4976.
(50) Yang, X.; Kang, S.; Yang, Y.; Aou, K.; Hsu, S. L. *Polymer* **2004**, *45*, 4241–4248.
(51) Zhang, J.; Duan, Y.; Domb, A. J.; Ozaki, Y. *Macromolecules* **2010**, *43*, 4240–4246.
(52) Na, B.; Lv, R. H.; Zou, S. F.; Li, Z. J.; Tian, N. N.; Fu, Q. *Macromolecules* **2010**, *43*, 1702–1705.
(53) Cho, J.; Baratian, S.; Kim, J.; Yeh, F.; Hsiao, B. S.; Runt, J. *Polymer* **2003**, *44*, 711–717.
(54) Kolstad, J. J. *J. Appl. Polym. Sci.* **1996**, *62*, 1079–1091.
(55) Zhang, J.; Tashiro, K.; Tsuji, H.; Domb, A. J. *Macromolecules* **2008**, *41*, 1352–1357.
(56) Yasuniwa, M.; Tsubakihara, S.; Sugimoto, Y.; Nakafuku, C. *J. Polym. Sci., Polym. Phys.* **2004**, *42*, 25–32.
(57) Solarski, S.; Ferreira, M.; Devaux, E. *Polym. Commun.* **2005**, *46*, 11187–11192.
(58) Yasuniwa, M.; Sakamo, K.; Ono, Y.; Kawahara, W. *Polymer* **2008**, *49*, 1943–1951.
(59) Na, B.; Tian, N. N.; Lv, R. H.; Li, Z. J.; Xu, W. F.; Fu, Q. *Polymer* **2010**, *51*, 563–567.